Histomorphometry and cortical robusticity of the adult human femur

Justyna Jolanta Miszkiewicz[1,2*], Patrick Mahoney[2]

[1]Skeletal Biology and Forensic Anthropology Research Group, School of Archaeology and Anthropology, Australian National University, 2601 Canberra, ACT, Australia

[2]Human Osteology Research Lab, Skeletal Biology Research Centre, School of Anthropology and Conservation, University of Kent, CT2 7NR Canterbury, Kent, United Kingdom

***Corresponding author:**

Justyna.Miszkiewicz@anu.edu.au

ABSTRACT

Recent quantitative analyses of human bone microanatomy, as well as theoretical models that propose bone micro- and gross anatomical associations, have started to reveal insights into biological links that may facilitate remodeling processes. However, relationships between bone size and the underlying cortical bone histology remain largely unexplored. The goal of this study is to determine the extent to which static indicators of bone remodeling and vascularity, measured using histomorphometric techniques, relate to femoral midshaft cortical width and robusticity. Using previously published and new quantitative data from 450 adult human male (n = 233) and female (n = 217) femora, we determine if these aspects of femoral size relate to bone microanatomy. Scaling relationships are explored and interpreted within a context of tissue form and function. Analyses revealed that the area and diameter of Haversian canals and secondary osteons, and densities of secondary osteons and osteocyte lacunae from the sub-periosteal region of the posterior midshaft femur cortex were significantly, but not consistently, associated with femoral size. Cortical width and bone robusticity were correlated with osteocyte lacunae density and scaled with positive allometry. Diameter and area of osteons and Haversian canals decreased as the width of cortex and bone robusticity increased, revealing a negative allometric relationship. These results indicate that measures of cortical bone remodeling and vascularity products link to femur size. Allometric relationships between more robust human femora with thicker cortical bone and histological products of bone remodeling correspond with principles of bone functional adaptation. Future studies may benefit from combining bone histomorphometric data with measurements of bone macrostructure.

Keywords: bone histomorphometry, osteocyte lacunae, osteons, Haversian canals, femur, cortical bone, bone functional adaptation

Abbreviations: Cortical width (Ct.Wi), Cortical width robusticity index (Ct.Wi.RI), intact osteon density (N.On), fragmentary osteon density (N.On.Fg), osteon population density (OPD), osteon area (On.Ar), Haversian canal area (H.Ar) and diameter (H.Dm), osteocyte lacunae density (Ot.Dn), reduced major axis regression (RMA)

INTRODUCTION

Analyses of bone microstructure can offer insights into skeletal growth, metabolism and structure-function adaptive relationships [1-3]. More specifically, histomorphometric examination yields remodeling data that can be evaluated in relation to mechanical loading history, diet, and disease [e.g. 4-7], and has been of particular importance in studies investigating the relationship between ontogeny, age-related disease, and bone modeling and remodeling [e.g. 8-10]. Recently, one of us [2] reported significant positive and negative correlations between different static histomorphometry variables that relate to bone remodeling associated with mechanical stimuli. Yet, relationships between bone gross anatomy and the underlying bone microstructure remain largely unexplored. Therefore, the present study builds upon this previous work, and examines midshaft femur size against histomorphometric data [2]. Our goal is to investigate the extent to which static histomorphometric evidence of cortical bone remodeling and vascularity relates to midshaft cortical width (Ct.Wi)[1], and a femoral robusticity index (Ct.Wi.RI) calculated from Ct.Wi data. We aim to provide insights into the complex relationship between outer and inner bone anatomy in relation to biological (metabolic and functional) processes. The modern human sample in our study is unique, deriving from a large well preserved recent archaeological skeletal collection curated at the University of Kent (UK). Usually, except for diagnostic bone biopsies taken from patients [e.g. 12], research into cortical histomorphometric variation in humans relies on smaller samples of cadavers [e.g. 5-7], or comparative experimental studies utilising non-human animal models [e.g. 8]. In addition to revealing the relationship between the size of a femur and the underlying products of bone remodeling, the present study extends previously reported human cortical histomorphometric data and findings [2].

[1]For the sake of clarity, and to ensure that our study follows standard histomorphometry nomenclature [11], we refer to the cortical distance between the endosteum and periosteum as "cortical width" (defining transverse 2D measurements of diaphyseal cortex) rather than "cortical thickness" (implying 3D measurements) [e.g. 24].

Form and function of limb long bones

The biomechanical properties of lower limb long bone diaphysis are best explained using basic structural engineering principles [13-14]. Large mechanical stress sustained by the human leg will be accommodated by periosteal expansion, strengthening bone tissue and minimising fracture risk [15]. Previous experimental studies have demonstrated bone enlargement under dynamic and/or repetitive mechanical loading regimes, and a decline in bone mass when load bearing is removed [e.g. 16-17]. Based upon these types of correlations, cross-sectional thickness or width of the cortex, robusticity index, measures of area moments of inertia, or simple cross-sectional geometry, have all served as proxies for the functional adaptation of the human femur [see 18 for evaluation].

At the histological level, when examined in a transverse plane, products of cortical remodeling may be informative of functional adaptation [e.g. 1-3, 7]. These include geometric properties (e.g. surface area, diameter, shape circularity) of secondary osteons (hereafter "osteons") and Haversian canals (indicative of bone vascularity), as well as densities of osteons and osteocyte lacunae [19]. By summing the number of fragmentary and intact osteons, a total osteon population density can be estimated for an examined section area, indicating an average number of bone remodeling products, serving as a proxy for bone density [2, 19]. Similarly, osteocytes (in living bone), or osteocyte lacunae (in preserved ancient bone) can be totalled per section area to indicate average density and, by extension, reflect an approximate rate of osteocyte proliferation [2, 20]. These variables may then be linked to bone functional adaptation given the mechanosensing properties of osteocytes [21]. Relatively smaller or larger osteon and Haversian canal area and diameter measurements represent transverse cross-sectional surfaces of bone microstructure, and may indicate how fast or slowly, and/or frequently cortical bone is filled by Basic Multicellular Units (BMUs) [22]. Indeed, previous human and non-human animal research demonstrated higher osteon and osteocyte lacunae densities, and smaller osteons and Haversian canals at bone sites associated with larger strain, mechanical stress, or type (direction) of mechanical load [e.g. 22-28].

Given that modeling of the human skeleton ceases almost completely with the onset of adulthood, information about the underlying remodeling activity can be mainly accessed using microscopic methods. Although it is estimated that only an approximate 30% of overall

remodeling activity relates to micro-damage repair [29], the accumulation of bone remodeled in response to function should manifest differently when evaluating the same bone type, of different sizes. However, limited empirical research has been undertaken investigating direct bone macro- and microscopic scaling relationships in human bone. Recent mathematical theoretical models of remodeling demonstrated that mean biomechanical stress nonuniformity has an important role in trabecular bone functional adaptation [30]. Experimentally, initial links have been identified between bone robusticity and cortical remodeling, warranting further investigation [31-34]. For example, using multiple methods applied to ten human cadaveric tibiae, Goldman et al [31] showed that bone robusticity had an effect on cortical remodeling by increasing the numbers and size of osteons. It was suggested that remodeling may be subject to global signalling that influences bone robusticity. Another recent study [32] demonstrated that differences in bone mass attainment due to sexual dimorphism may not be entirely representative of the classic perception that females attain more slender bones than males. Using a large sample (n = 241) of femora derived from an anthropological skeletal collection, Jepsen et al. [32] showed that, in fact, bone mass is relative to sex-specific body and bone size. This is supported by an earlier study suggesting similar bone mechanical properties for different bone size in males and females [33]. Finally, using 115 adult human long bones, Schlecht and Jepsen [34] indicated a co-variance between bone robusticity and strength/stiffness, highlighting that meaningful analyses of skeletal traits may be best achieved when multiple aspects of bone functional adaptation (e.g. size, volume, stiffness) are considered together. Therefore, these studies have begun to indicate clear relationships between bone microanatomy and gross morphology. Recently, we [2] reported a series of positive and negative correlations between classic static histomorphometry variables representing products of cortical remodeling in the human midshaft femur. Here, these data are analysed in relation to femoral cortical width and its associated femoral robusticity in the same sample, extending the original findings. Two "themes" are investigated, exploring scaling relationships of bone metabolic and structural change:

Predictions:

a) Functional relationships - if femoral diaphyseal cortical properties are influenced and/or underlie mechanically induced remodeling, the following basic engineering

principles apply: (i) osteon and osteocyte lacunae densities should correlate with an increase in cortical width and femoral robusticity and scale with positive allometry, but (ii) osteon and Haversian canal size and diameter should correlate with an increase in cortical width and femoral robusticity and scale with negative allometry.

b) Dimensional relationships – if bone microstructure is a simple reflection of the intra-specific variation in femur size (i.e. "naturally" larger vs. "naturally" smaller bone), then all histology variables should increase in size or density at proportionally the same rate as cortical width and femoral robusticity increase in size. Under this scenario, the growth ratio between the variables will be isometric.

MATERIALS AND METHODS

Data used in our study derive from a skeletal sample (n = 450) of British modern human adult remains curated in the Skeletal Biology Research Centre at the University of Kent (UK). These remains were recovered from one site and have been dated to between 900 to 400 years ago [24]. Examination of this skeletal material followed standard permissions and anthropological codes of practice and ethics[2]. Given the historical context of this sample, Human Tissue Act(s) regulations do not pertain to our study.

Individuation procedures

Standard anthropological methods of age-at-death and sex estimation were followed to reconstruct the biological profile of each adult [35]. A total of 450 adults was separated into age and sex sub-groups, resulting in: 217 females, 233 males, 126 young (20 – 35 years old) and 319 middle-aged adults (35 – 50 years old), and 5 old adults (50+ years old) (four males, and one female).

[2]Code of Ethics of the American Association of Physical Anthropologists (2003) http://physanth.org/documents/3/ethics.pdf, British Association for Biological Anthropology and Osteoarchaeology Code of Practice (2010) http://www.babao.org.uk/index/ethics-and-standards, Mays S, Elders J, Humphrey L, White W, and Marshall P (2013) Science and the Dead: guidelines for the destructive sampling of archaeological human remains for scientific analysis. Advisory Panel on the Archaeology of Burials in England. English Heritage.

Further sub-divisions were made into 49 young males and 77 young females, 139 middle-aged females, and 180 middle-aged males (Table 1). Due to the small sample size, individuals in the

"old" age category (aged 50 or more years) were excluded from analyses that controlled for age.

Macroscopic and microscopic femoral examination

The process of femoral midshaft sectioning, and thin section preparation in this sample has been previously described elsewhere [e.g. 2, 24]. The thin sections were originally produced as part of a larger project [36]. In brief, right (n = 367) and left (n = 83) femora, selected from individuals with no evident skeletal pathology, were pooled due to a lack of data asymmetry. In order for the sectioning to be as minimally invasive as possible, the posterior quarter of midshaft diaphysis was extracted (approximately 1 ± 0.2 cm thick) and examined. The posterior femoral aspect was also chosen as a suitable sectioning location as it relates closely to lower limb behaviour (i.e. the sectioning location overlaps linea aspera). Prior to thin section preparation, Ct.Wi was recorded using standard digital calipers by placing the measuring needles on the most external surfaces of the endosteum and periosteum. Robusticity indices were calculated by dividing Ct.Wi data by maximum femoral length [18]. Thin section preparation followed standard procedures [see 2]. Samples were embedded in Buehler EpoxiCure® resin, cut on a precision saw, attached to microscope slides, ground and polished to reveal histology. This was followed by cleaning and dehydrating in a series of ethanol baths and covering with glass slips.

Some of the histology data examined here were previously analysed in other studies addressing questions that are not the focus of the present research [e.g. 2, 24, 37]. However, relationships between histomorphometric variables and femoral cortical width and robusticity are examined here for the first time. In brief, values of intact (N.On), fragmentary (N.On.Fg), and total osteon population density (OPD), as well as osteon area (On.Ar), Haversian canal area (H.Ar) and diameter (H.Dm), and osteocyte lacunae density (Ot.Dn) were recorded under a BX51 Olympus microscope with an Olympus DP25 camera. Additional imaging of thin sections (Figure 1) was undertaken using AmScope MU130 microscope digital camera and its associated AmScope (2016) software. A mean value was calculated for each variable from a maximum of six regions of interest (ROIs), extending along the sub-periosteal cortical region. Measurements and counts were performed in CELL® Live Biology Imaging software (Olympus). In some cases, the archaeological condition of samples meant it was

difficult to consistently select the exact same ROIs (e.g. due to localised bioerosion). However, data are in line with current standards (recommending 25 – 50 osteons to be evaluated per section), and were captured using a range of 2X, 4X, 10X, 20X, and 40X magnification [2].

Inferential statistics

Statistical analyses were undertaken using IBM SPSS Statistics 22.0® (2013), *R* (2.5.0, i386 3.4.0)® (2007), and Past3® [38]. Data were examined for: normal distribution (Kolmogorov-Smirnov or Shapiro Wilk tests depending on sample size within age and sex groupings), intra-observer error (n = 45), and data asymmetry between right and left femora (independent samples *t*-test) [36]. The macro-microscopic associations were investigated in two stages. Simple correlations were performed first, Reduced Major Axis (RMA) regressions were undertaken second. In both stages, cortical width, and robusticity indices, were considered independent variables and thus plotted on the x axis. This is because our research questions centre on determining the extent to which histology (y axis) depends on macrostructure. However, it is noted that a RMA regression does not require a well defined mutual relationship between the two variables [39]. In fact, it is acceptable to use RMA in tests which include somewhat arbitrary, but co-dependent x and y variable interaction [39]. This is a suitable approach in the present study, given there may never be absolute certainty as to whether, universally, bone robusticity influences histology, or histology determines bone robusticity.

Firstly, due to skewed raw data, the simple correlations were sought using non-parametric Spearman's tests in the entire sample, and then repeated within each of the age and sex sub-groups. The strength of each correlation was evaluated by the value of r^2 (coefficient of determination) with coefficients equal to or larger than 20% - 40% being deemed weak to moderate correlations [40]. Here, scattergrams for the three strongest correlations are presented (Figures 2-3), and results are interpreted only for r^2 values equal to higher than 20%. All results are presented in tables (Tables 2-5; Supplement Tables 2-3). A line of best fit is included in the Scattergrams (Figures 2-3) to visualise the direction in data change. Given the skewness of raw data, we also fitted each plot with a loess line to illustrate monotonic downward or upward trend(s) in data [41]. As previously documented [2, 24], no intra-observer error was identified, but there were inconsistent patterns in histology data

distribution (i.e. fluctuating between normal and abnormal within age and sex sub-groups), and though transformed for the purpose of parametric testing in our previous studies [e.g. 2, 24], raw data were analysed here via non-parametric tests. This was necessary because of the new addition of macroscopic cortical width measurements, and flexibility in making no assumptions about the underlying data distribution in the broader (or interpretive) context of bone metabolism. The correlations were performed on every single histology variable, along with additional four histology "ratio" variables (presented in the Supplement):

- H.Ar: On.Ar - indicating how much of lamellar wall per osteon there is per section, along with any mutual, accompanying changes in the size of Haversian canal and osteon surface area (the higher the ratio value, the larger the microstructural unit, and the thinner the lamellar portion of osteons);
- N.On: OPD - indicating a biological correspondence of intact osteons to total osteon population (the higher the value, the denser the bone section in unremodeled osteons);
- Ot.Dn: OPD – indicating a biological correspondence of osteocyte lacunae to total osteon population (the higher the value, the denser the bone section);
- Ot.Dn: On.Ar – indicating a biological correspondence of osteocyte lacunae to osteon surface area (a value of 1 would suggest a tight relationship between osteon size and cell density, and thus disprove the hypothesized opposite effect of biomechanical stimulation upon cortical histomorphometry).

Secondly, regression of log-transformed data were conducted through RMA analysis to examine the growth ratio between the variables. This statistical model accounts for variation in data plotted on both the x and y axis (given these are data from deceased humans, and bone remodeling rates vary intra-specifically) [39, 42]. Additionally, the RMA regression is symmetrical, whereby deviations in x and y data are minimized [38]. Macrostructure data on the x axis were regressed against histology (and ratio) data on the y axis. The RMA regression results were evaluated based on slope (b), r^2 (coefficient of determination), the 95% slope confidence interval (95% CI), intercept, and significance (p) values. Scattergrams representing the three strongest RMA regression results are presented (Figures 2-3), and all results are reported in Tables 4-5 (along with Supplement Table 3). The RMA regressions were only undertaken on the strongest initial correlations identified in the first step of the analysis

(Tables 2-3, Supplement Table 2). Isometric macro-microscopic growth is identified when/if *b* equals 1. This means that the growth ratio between femoral size and the underlying microscopic structures is constant, indicating a dimensional anatomical effect. Negative or positive allometry is identified when/if *b* is < 1, or > 1 respectively, which is also evaluated through the 95% CI's. This means that the growth ratio between femoral size and the underlying microscopic structures is not constant, and one increases at a proportionally faster/slower rate that the other. When viewed alongside our predictions, this indicates a bone functional adaptation effect.

RESULTS

Descriptive statistics for histology data were previously published in [2] and partly in [23, 37]. Descriptive data for the new Ct.Wi and Ct.Wi.RI variables are given in Table 1, whereas histology ratio data appear in the Supplement Table 1. Results from the inferential analysis are presented in Tables 2-5, and Supplement Tables 2-3. Out of 198 correlation tests performed, 145 (~73%) were statistically significant at $p < .05$ (Tables 2-3, Supplement Table 2). Using Ct.Wi data only (99 tests), 70 (~71%) were statistically significant (*p* range from 0.000 to 0.048) (Table 2, Supplement Table 2, Figures 2-3). Twelve of those were of moderate strength (*r* range from -0.596 to -0.432). Further 29 significant correlations were weak, explaining more than 10% but less than 20% of data variation. The remaining significant results failed to explain substantial portions of data (< 10%), though some general trends in data were still identified.

Subsequent analyses, where femoral robusticity calculated from Ct.Wi was assessed against the histology variables (repeated 99 tests), revealed 75 (~76%) statistically significant (*p* range from 0.000 to 0.046) correlations (Table 3, Supplement Table 2, Figure 3). Seven of which were also of moderate strength (*r* range from -0.517 to 0.424). There were 34 weak significant correlations (explaining > 10% but < 20% of data variation), and the remaining significant correlations failed to explain > 10% of data variation. Therefore, there was a slight improvement in the number and strength of the relationships between Ct.Wi.RI, and the histomorphometric variables (Table 3; Supplement Table 2, Figure 3).

Reduced Major Axis regression analyses revealed consistent relationships between femoral cortical width and the size of the histology variables. The relationship of Haversian canal size (area and diameter), and the relationship of osteon area, to cortical width is negatively allometric (Tables 4-5; Figures 2-3; Supplement Tables 1-3). Thus, individuals with smaller Haversian canals, and smaller osteons, have a relatively greater cortical width, compared to individuals with thinner femoral cortical bone. The scaling relationship between our measure of femoral size and the histology frequency and density variables is less consistent. The relationship of intact osteon density and osteon population density to cortical width is isometric, while osteocyte lacunae density and cortical width scale with positive allometry. This implies that the frequency of osteons and cortical width increase or decrease in number or size at relatively equivalent rates. In contrast, individuals with fewer osteocyte lacunae have relatively thinner femoral cortical bone, but individuals with thicker femoral cortices have a proportional greater density of osteocyte lacunae. This latter pattern occurs because osteocytes accumulate at a faster rate than the relative increase in femoral cortical width. Thus, individuals with thicker cortical bone at the posterior quarter of the midshaft diaphysis have a greater density of osteons, but they also have a *proportionally* greater density of osteocyte lacunae. Overall, RMA regression analyses have revealed biological scaling relationships whereby individuals with thicker cortices have *relatively* smaller Haversian canals and osteons combined with a greater density of osteocyte lacunae, compared to individuals with thinner femoral cortices.

DISCUSSION

The aim in this study was to investigate structural relationships between measures of cortical width and robusticity, and histomorphometric variation in the human midshaft femur. Two predictions were tested, evaluating whether macro- and microstructural cortical bone associations can be explained from (1) functional and/or (2) dimensional perspectives. Our analyses reveal that, on average, relative changes in histomorphometric measures of bone remodeling products (i.e. secondary osteon tissue) occur in an association with equivalent changes in femoral cortical width. These associations are fairly consistent, with a directional, allometric, relationship between cortical bone micro- and macro- structures. As age and sex variation was accounted for in our study (when undertaking statistical analyses within the

sub-groups), these findings support the idea that bone functional adaptation may play a major role in the structural design of femur diaphysis. However, it is impossible to completely rule out inherent intra-specific sex and age variation in human bone metabolism given that this study utilises histomorphometry data from archaeological humans. Our data provide a basis from which to investigate these scaling and functional effects further in experimental contexts.

Functional prediction

Our data are compatible with a biomechanical explanation of femur size and structure. Osteon and Haversian canal size became smaller with an increase in cortical width and/or robusticity. However, these trends were not consistent across the entire sample. For example, not only was fragmentary osteon density not significantly associated with Ct.Wi or Ct.Wi.RI, its *r* coefficient also fluctuated between positive and negative between and within age and sex (sub)groups (Tables 2-5, Supplement Table 2). This may be due to the effects of aging and/or sex specific factors underlying bone remodeling in adults. In all other instances, where results were not significant, the biomechanical prediction was mainly supported.

The gross structure and geometric properties of a long bone diaphysis are indicators of functional adaptation, and are modeled predominantly during the child and adolescent stages of ontogeny [10, 15, 43]. In most cases, once adulthood is reached, optimal mechanical loading is accommodated by targeted remodeling of accrued localised micro-damage by replacing and/or adding new bone [29]. Through a series of positive and negative correlations, along with tests for allometry, the present study supports this functional adaptation of structure in the midshaft human femur. These results agree with basic engineering predictions, and support previous studies of cortical histomorphometric change in relation to strain or mechanical load [e.g. 7, 22-28, 44]. However, it is noted that the sample utilised here relies on mechanical loading inferences through simple measures of bone robusticity. Variation in correlations between the age and sex groups indicates relationships between cortical size and the underlying microstructure are not consistent (Tables 2-5; Supplement Tables 2-3), supporting the well established intra-specific differences in human bone metabolic activity [5]. There is no doubt that individuals in our sample represent a variety of physical activity regimes. There seems to be a clear functional signal in the results in the young

male category, potentially suggesting higher intensity and/or frequency of mechanical load experienced by this group [see 24 for review of behaviours potentially represented by this sample].

Dimensional prediction

The study of allometry in biology has long had important implications for our understanding of structural and functional tissue relationships [45]. It has been of particular importance in studies examining mechanical adaptation of mammalian trabecular bone [46]. However, as identified recently, the assumption that simple intra-specific variation in human skeletal size may be considered to play a role in determining microstructural geometric or other quantitative bone data, is rarely accounted for in research. The present study revealed an isometric relationship between osteon density and cortical robusticity, which supports the idea that larger femora maintain more frequent osteons. However, if only this type of relationship explains the changes in histomorphometric data that accompanies increases in femoral robusticity, then it is unclear why the more robust femora also revealed allometric scaling relationships with bone microstructure. Both Goldman et al [31] and Schlecht and Jepsen [34] previously identified a link between micro- and macro-structure of bone. Our results support their findings, but also highlight the potential effect of localised remodeling on histomorphometry. Similarly to our findings, Goldman et al [31] noted that robust tibiae appear to have more numerous osteons. This micro-macro effect in our study was not consistent across the sample, indicating potential mechanically-induced remodeling may obscure otherwise clear robusticity related relationships. Goldman et al's study [31] examined human tibiae from two different midshaft locations allowing for a broader examination and intra-bone comparison of intra-cortical remodeling, whereas our study focused on sub-periosteal histology from the posterior femoral midshaft only. Thus, the different findings from the two studies are most certainly underlied by variation in sampling location, indicating that remodeling is not constant across intra- and inter-specific cortical sites, bones, and individuals.

Bone structural relationships at the macroscopic and microscopic level are complex

Using geometric properties of osteons and Haversian canals, which are inversely related to strain, our osteon density data could be simply interpreted in a broader mechanical context.

While our results support structural bone functional adaptation, it is difficult to exclude the scaling effect of cortical size on histological parameters. This is most clear for osteon densities. Both the intact and total population densities increased in value along with an increase in cortical width and robusticity, which in principle agrees with the first part of both predictions evaluated here. However, given that fragmentary osteon density data did not follow our predictions, and were not significantly correlated with cortical width and/or robusticity either, this may reflect difficulty in distinguishing between scaling versus functional adaptation relationships at the human midshaft femur. This relationship is likely to be further complicated by the effect of aging and sex on the fragmentary osteon density data across the sample. Whilst our RMA regressions attempt to address this, they explain only a portion of the entire data-set, encouraging future research to collect more data. Fragmentary osteon density is a valid proxy for cortical products of bone remodeling because they are remnants of preceding or pre-exisiting intact osteons [19]. Their increased presence can indicate a higher proportion of cortical bone being remodeled and filled with new osteons. By examining the *r* coefficients of variation (Tables 2-3), fragmentary osteons were positively correlated with cortical width and robusticity in the entire sample, young adults, middle-aged adults, and young males. The relationship was negative in all the remaining sub-groups. This, however small, deviation from the rest of the results highlights the complexity of functional, structural, and metabolic activity in bone.

It is now well established that there is a complementary interaction between genetic, hormonal, dietary, and mechanical factors in regulation of bone remodeling [15]. Of course the results from our skeletal collection do not account for the broad biological picture of bone metabolism. We acknowledge that the standard anthropological age categories are relatively broad and thus may relate to minor osteon number variation with age [47]. In our previous study [24], we also reported histomorphometric variation with social status in this sample related to documented lifestyles [see also 48]. Our conclusions were supported by an evaluation of histological variation adjusted by femoral robusticity index based on midshaft circumference. This showed that femora of similar size in age- and sex- matched humans have different remodeling activity when related to a known behavioural context. Given that the aim in the present study was to seek structural biology relationships (rather than undertaking group comparisons), our present results support these previous conclusions. The complexity

of factors behind cortical bone remodeling thus makes it difficult to characterise either biomechanical or dimensional relationships between macro- and microstructure - they are probably complimentary or dependent upon individual/ populational aspects of biology and/or lifestyle. We further acknowledge that it was not possible to measure collagen and mineral content in our study, bone components which are important in facilitating mechanical adaptation [49]. Our finding has methodological implications whereby it seems that data collected either macro- or microscopically alone, may not reflect the complexity of bone form and function relationships.

CONCLUSIONS

This study demonstrates a relationship between femoral size and the underlying histological products of bone growth. The density of osteons, and osteocyte lacunae, increased in more robust femora, and in those with thicker cortical bone. Allometric scaling relationships were also observed. More robust femora with thicker cortical bone also had smaller osteons and Haversian canals, and scaled with negative allometry. These data are compatible with the idea that human femoral macroscopic and microscopic structures are driven by functional adaptation. It is suggested that cortical histomorphometry data examined in future research may benefit from an examination in the light of macroscopic structural measures. Studies aiming to unravel functional adaptation from bone should ideally undertake an integrative approach of macro- (robusticity, size, geometric properties), microscopic (e.g. histological parameters), and strength/ stiffness (mineral density, collagen orientation) variables. Only then a more complete human femur form and function relationship will be understood [50].

ACKNOWLEDGMENTS

We thank the School of Anthropology and Conservation (University of Kent, UK) for research funding (JJM), The Royal Society for equipment funding (PM), Prof Kate Robson Brown (Bristol), Prof Richard Griffiths (Kent), and Prof Dr David Roberts (Kent) for research support, and Prof Stephen Haslett (ANU), Dr Simon Tollington (Kent), Alannah Pearson (ANU), Dr Julien Louys (ANU) for statistical advice. Invaluable feedback from the editor and two reviewers greatly improved our manuscript.

REFERENCES CITED

1. Cambra-Moo O, Nacarino-Meneses C, Díaz-Güemes I, Enciso S, Gil OG, Rodríguez LL, Angel Rodríguez MÁ, Antonio BH (2015) Multidisciplinary characterization of the long-bone cortex growth patterns through sheep's ontogeny. J Struct Biol 191: 1-9.
2. Miszkiewicz JJ (2016) Investigating histomorphometric relationships at the human femoral midshaft in a biomechanical context. J Bone Miner Metab 34: 179-192.
3. Skedros JG, Su SC, Bloebaum RD (1997) Biomechanical implications of mineral content and microstructural variations in cortical bone of horse, elk, and sheep calcanei. Anat Rec 249: 297–316.
4. Bourrin S, Ghaemmaghami F, Vico L, Chappard D, Gharib C, Alexandre C, (1992) Effect of a five-week swimming program on rat bone: a histomorphometric study. Calcif Tissue Int 51: 137-142.
5. Britz HM, Thomas CDL, Clement JG, Cooper DML (2009) The relation of femoral osteon geometry to age, sex, height and weight. Bone 45: 77–83.
6. Dempster DW, Cosman F, Kurland ES, Zhou H, Nieves J, Woelfert L, Shane E, Plavetić K, Müller R, Bilezikian J, Lindsay R (2001) Effects of daily treatment with parathyroid hormone on bone microarchitecture and turnover in patients with osteoporosis: a paired biopsy study. J Bone Miner Res 16: 1846-1853.
7. Schlecht SH, Pinto DC, Agnew AM, Stout SD (2012) Brief communication: The effects of disuse on the mechanical properties of bone: What unloading tells us about the adaptive nature of skeletal tissue. Am J Phys Anthropol 149: 599-605.
8. Li XJ, Jee WSS, Ke HZ, Mori S, Akamine T (1991) Age-related changes of cancellous and cortical bone histomorphometry in female Sprague-Dawley rats. Cells Mater 1: 25-25.
9. Rauch F, Travers R, Parfitt AM, Glorieux FH (2000) Static and dynamic bone histomorphometry in children with osteogenesis imperfecta. Bone 26: 581-589.
10. Pitfield R, Miszkiewicz JJ, Mahoney P (2017) Cortical histomorphometry of the human humerus during ontogeny. Calc Tiss Int 101: 148-158.
11. Dempster DW, Compston JE, Drezner MK, Glorieux FH, Kanis JA, Malluche H, Meunier PJ, Ott SM, Recker RR, Parfitt AM (2013) Standardized nomenclature, symbols, and units for bone histomorphometry: A 2012 update of the report of the ASBMR Histomorphometry Nomenclature Committee. J Bone Miner Res 28: 2-17.
12. Chavassieux PM, Arlot ME, Roux JP, Portero N, Daifotis A, Yates AJ, Hamdy NAT, Malice M, Freedholm D, Meunier PJ (2000) Effects of Alendronate on Bone Quality and Remodeling in Glucocorticoid-Induced Osteoporosis: A Histomorphometric Analysis of Transiliac Biopsies. J Bone Miner Res 15: 754-762.
13. Athanasiou KA, Zhu CF, Lanctot DR, Agrawal CM, Wang X (2000) Fundamentals of biomechanics in tissue engineering of bone. Tiss Eng 6: 361-381.
14. Frost HM (1987b) Bone "mass" and the "mechanostat": A proposal. Anat Rec 219: 1–9.
15. Robling AG, Castillo AB, Turner CH (2006) Biomechanical and molecular regulation of bone remodeling. Annu. Rev Biomed Eng 8: 455-498.

16. Lanyon LE, Goodship AE, Pye CJ, MacFie JH (1982) Mechanically adaptive bone remodeling. J Biomech 15: 141–54.
17. Moustafa A, Sugiyama T, Saxon LK, Zaman G, Sunters A, Armstrong VJ, Javaheri B, Lanyon LE, Price JS (2009) The mouse fibula as a suitable bone for the study of functional adaptation to mechanical loading. Bone 44: 930-935.
18. Stock JT, Shaw CN (2007) Which measures of diaphyseal robusticity are robust? A comparison of external methods of quantifying the strength of long bone diaphyses to cross-sectional geometric properties. Am J Phys Anthropol 134: 412-423.
19. Stout S, Crowder C. (2011) Bone Remodeling, Histomorphology, and Histomorphometry. In Crowder C, Stout SD (Eds) Bone Histology: An Anthropological Perspective, Boca Raton, FL: CRC Press, pp. 1–21.
20. Bromage TG, Juwayeyi YM, Katris JA, Gomez S, Ovsiy O, Goldstein J, Janal MN, Hu B, Schrenk F (2016) The scaling of human osteocyte lacuna density with body size and metabolism. Comptes Rendus Palevol 15: 33-40.
21. Klein-Nulend J, Bakker AD, Bacabac RG, Vatsa A, Weinbaum S (2012) Mechanosensation and transduction in osteocytes. Bone 54: 190–182.
22. Van Oers RFM, Ruimerman R, Van Rietbergen B, Hilbers PAJ, Huiskes R (2008) Relating osteon diameter to strain. Bone 43: 476–82.
23. Britz HM, Jokihaara J, Leppänen OV, Järvinen TL, Cooper DM (2012) The effects of immobilization on vascular canal orientation in rat cortical bone. J Anat 220: 67-76.
24. Miszkiewicz JJ, Mahoney P (2016) Ancient human bone microstructure in medieval England: comparisons between two socio-economic groups. Anat Rec 299: 42-59.
25. Skedros JG, Mason MW, Bloebaum RD. (1994) Differences in osteonal micromorphology between tensile and compressive cortices of a bending skeletal system: Indications of potential strain-specific differences in bone microstructure. Anat Rec 239: 405-413.
26. Wojda SJ, Weyland DR, Gray SK, Mcgee-Lawrence ME, Drummer TD, Donahue SW (2013) Black bears with longer disuse (hibernation) periods have lower femoral osteon population density and greater mineralization and intracortical porosity. Anat Rec 296: 1148-1153.
27. Sugawara Y, Kamioka H, Ishihara Y, Fujisawa N, Kawanabe N, Yamashiro T. (2013) The early mouse 3D osteocyte network in the presence and absence of mechanical loading. Bone 52: 189-196.
28. Totland GK, Fjelldal PG, Kryvi H, Løkka G, Wargelius A, Sagstad A, Hansen T, Grotmol S (2011) Sustained swimming increases the mineral content and osteocyte density of salmon vertebral bone. J Anat 219: 490–501.
29. Martin RB (2002) Is all cortical bone remodeling initiated by microdamage? Bone 30: 8-13.

30. Kim YK, Kameo Y, Tanaka S, Adachi T (2017) Capturing microscopic features of bone remodeling into a macroscopic model based on biological rationales of bone adaptation. Biomech Model Mechanobiol (Online First).
31. Goldman HM, Hampson NA, Guth JJ, Lin D, Jepsen KJ (2014) Intracortical remodeling parameters are associated with measures of bone robustness. Anat Rec 297: 1817-1828.
32. Jepsen KJ, Bigelow EM, Schlecht SH (2015) Women build long bones with less cortical mass relative to body size and bone size compared with men. Clin Orthop Relat Res 473: 2530–2539.
33. Tommasini SM, Nasser P, Jepsen KJ (2007) Sexual dimorphism affects tibia size and shape but not tissue-level mechanical properties. Bone 40: 498–505.
34. Schlecht SH, Jepsen KJ (2013) Functional integration of skeletal traits: an intraskeletal assessment of bone size, mineralization, and volume covariance. Bone 56: 127-138.
35. Buikstra JE, Ubelaker DH (1994) Standards for data collection from human skeletal remains. Fayetteville: Arkansas Archaeology Survey.
36. Miszkiewicz JJ (2014) Ancient Human Bone Histology and Behaviour. University of Kent, PhD Thesis.
37. Mahoney P, Miszkiewicz JJ, Chapple S, Le Luyer M, Schlecht SH, Stewart TJ, Griffiths RA, Deter C, Guatelli Steinberg D (2017) The biorhythm of human skeletal growth. J Anat (early view)
38. Hammer Ø, Harper DAT, Ryan PD (2001) PAST-palaeontological statistics, ver. 1.89. Palaeont Electr 4(9).
39. Smith RJ (2009) Use and misuse of the reduced major axis for line-fitting. Am J Phys Anthropol 140: 476-486.
40. Taylor R (1990) Interpretation of the correlation coefficient: a basic review. J Diagn Med Sonogr 6: 35-39.
41. Breitling LP (2015) Calcium intake and bone mineral density as an example of non-linearity and threshold analysis. Osteoporosis Int 26: 1271-1281.
42. Warton DI, Wright IJ, Falster DS, Westoby M (2006) Bivariate line-fitting methods for allometry. Biol Rev 81: 259-291.
43. Pearson OM, Lieberman DE (2004) The aging of Wolff's “law”: ontogeny and responses to mechanical loading in cortical bone. Am J Phys Anthropol 125: 63-99.
44. LaMothe JM, Hamilton NH, Zernicke RF (2005) Strain rate influences periosteal adaptation in mature bone. Med Eng Phys 27: 277-284.
45. Thompson DW (1942) On growth and form. Cambridge University Press.
46. Barak MM, Lieberman DE, Hublin JJ (2013) Of mice, rats and men: trabecular bone architecture in mammals scales to body mass with negative allometry. J Struct Biol 183: 123-131.
47. Thompson DD, Galvin CA (1983) Estimation of age at death by tibial osteon remodeling in an autopsy series. Foren Sci Int 22: 203-211.

48. Nowlan NC, Jepsen KJ, Morgan EF (2011) Smaller, weaker, and less stiff bones evolve from changes in subsistence strategy. Osteoporosis Int 22: 1967–1980.
49. Yerramshetty JS, Akkus O (2008) The associations between mineral crystallinity and the mechanical properties of human cortical bone. Bone 42: 476-48.
50. Currey JD (2003) The many adaptations of bone. J Biomech 36: 1487-1495.

Table 1. Descriptive data for posterior cortical width (Ct.Wi in mm) and femoral robusticity index (Ct.Wi.RI = Ct.Wi/ Max.L x 100).

Ct.Wi groupings	**N**	**Min**	**Max**	**Mean**	**SD**
Entire sample*	450	4.83	15.73	8.98	1.79
Females	217	4.83	12.08	8.35	1.51
Males	233	5.03	15.73	9.57	1.84
Young adults	126	4.83	13.35	8.71	1.77
Middle-aged adults	319	5.03	15.73	9.08	1.80
Old adults	5	6.84	10.65	9.44	1.55
Young females	77	4.83	12.08	8.06	1.58
Middle-aged females	139	5.22	11.79	8.52	1.45
Old females	1	6.84	6.84	6.84	-
Young males	49	6.01	13.35	9.73	1.58
Middle-aged males	180	5.03	15.73	9.51	1.92
Old males	4	9.32	10.65	10.09	.64
Ct.Wi.RI groupings					
Entire sample*	423	1.10	3.89	2.05	.40
Females	206	1.13	2.92	1.99	.37
Males	217	1.10	3.89	2.11	.41
Young adults	116	1.13	3.89	2.04	.41
Middle-aged adults	303	1.10	3.53	2.05	.39
Young adults	4	2.09	2.42	2.30	.14
Young females	71	1.13	2.92	1.94	.37
Middle-aged females	135	1.17	2.90	2.01	.37
Young males	45	1.28	3.89	2.19	.43
Middle-aged males	168	1.10	3.53	2.09	.41
Old males	4	2.09	2.42	2.30	.14

*portion of data from [24: 51-52]

Table 2. Results from Spearman's correlation tests evaluating histomorphometry data against posterior cortical width (Ct.Wi). Underlined r^2 results indicate weak to moderate correlations, whereas the *p* values in bold indicate statistical significance < 0.05.

Variable correlated with Ct.Wi	Statistic	Entire Sample	Females	Males	Young adults	Middle-aged adults	Young females	Young males	Middle-aged females	Middle-aged males
N.On	*r*	.288	.216	.286	.346	.249	.215	.399	.191	.255
	r^2	8.29%	4.67%	8.18%	11.97%	6.20%	4.62%	15.92%	3.65%	6.50%
	p	**.000**	**.002**	**.000**	**.000**	**.000**	.063	**.005**	**.026**	**.001**
	n	443	213	230	124	314	76	48	136	178
N.On.Fg	*r*	.023	-.075	-.008	.021	.003	-.115	.213	-.070	-.032
	r^2	0.05%	0.56%	0.64%	0.04%	0.00%	1.32%	4.54%	0.49%	0.10%
	p	.647	.300	.903	.820	.953	.343	.155	.444	.674
	n	413	193	220	116	292	70	46	122	170
OPD	*r*	.257	.137	.223	.273	.241	.090	.461	.168	.195
	r^2	6.60%	1.88%	4.97%	7.45%	5.81%	0.81%	21.25%	2.82%	3.80%
	p	**.000**	.057	**.001**	**.003**	**.000**	.460	**.001**	.064	**.011**
	n	413	193	220	116	292	70	46	122	170
H.Ar	*r*	-.384	-.403	-.338	-.310	-.411	-.226	-.232	-.518	-.347
	r^2	14.75%	16.24%	11.42%	9.61%	16.89%	5.11%	5.38%	26.83%	12.04%
	p	**.000**	**.000**	**.000**	**.000**	**.000**	**.048**	.109	**.000**	**.000**
	n	450	217	233	126	319	77	49	139	180
H.Dm	*r*	-.451	-.437	-.409	-.412	-.465	-.284	-.402	-.539	-.398
	r^2	20.34%	19.10%	16.73%	16.97%	21.62%	8.07%	16.16%	29.05%	15.84%
	p	**.000**	**.000**	**.000**	**.000**	**.000**	**.012**	**.004**	**.000**	**.000**
	n	450	217	233	126	319	77	49	139	180
On.Ar	*r*	-.380	-.329	-.365	-.289	-.405	-.137	-.244	-.435	-.374
	r^2	14.44%	10.82%	13.32%	8.26%	16.40%	1.88%	5.95%	18.92%	13.99%
	p	**.000**	**.000**	**.000**	**.002**	**.000**	.267	.119	**.000**	**.000**
	n	401	190	211	110	286	68	42	121	165
Ot.Dn	*r*	.412	.348	.410	.447	.387	.234	.596	.405	.355
	r^2	16.97%	12.11%	16.81%	19.98%	14.98%	5.48%	35.52%	16.40%	12.60%
	p	**.000**	**.000**	**.000**	**.000**	**.000**	.080	**.000**	**.000**	**.000**
	n	353	161	192	96	252	57	39	103	149

Table 3. Results from Spearman's correlation tests evaluating histomorphometry data against posterior cortical width robusticity index (Ct.Wi.RI). Underlined r^2 results indicate weak to moderate correlations, whereas the *p* values in bold indicate statistical significance < 0.05.

Variable correlated with Ct.Wi.RI	**Statistic**	**Entire Sample**	**Females**	**Males**	**Young adults**	**Middle-aged adults**	**Young females**	**Young males**	**Middle-aged females**	**Middle-aged males**
N.On	*r*	.254	.264	.209	.344	.208	.281	.331	.234	.175
	r^2	6.45%	6.97%	4.37%	11.83%	4.33%	7.90%	10.96%	5.48%	3.06%
	p	**.000**	**.000**	**.002**	**.000**	**.000**	**.018**	**.028**	**.007**	**.024**
	n	416	202	214	114	298	70	44	132	166
N.On.Fg	*r*	-.008	-.041	-.030	.030	-.027	.004	.101	-.089	-.025
	r^2	0.01%	0.17%	0.09%	0.09%	0.07%	0.00%	1.02%	0.79%	0.06%
	p	.875	.584	.674	.761	.655	.972	.523	.338	.755
	n	387	182	205	106	277	64	42	118	159
OPD	*r*	.233	.236	.164	.342	.193	.270	.381	.211	.142
	r^2	5.43%	5.57%	2.69%	11.70%	3.72%	7.29%	14.52%	4.45%	2.02%
	p	**.000**	**.001**	**.019**	**.000**	**.001**	**.031**	**.013**	**.022**	.074
	n	387	182	205	106	277	64	42	118	159
H.Ar	*r*	-.385	-.416	-.331	-.343	-.395	-.292	-.299	-.492	-.318
	r^2	14.82%	17.31%	10.96%	11.76%	15.60%	8.53%	8.94%	24.21%	10.11%
	p	**.000**	**.000**	**.000**	**.000**	**.000**	**.014**	**.046**	**.000**	**.000**
	n	423	206	217	116	303	71	45	135	168
H.Dm	*r*	-.443	-.448	-.404	-.417	-.444	-.322	-.418	-.517	-.379
	r^2	19.63%	20.07%	16.32%	17.39%	19.71%	10.37%	17.47%	26.73%	14.36%
	p	**.000**	**.000**	**.000**	**.000**	**.000**	**.006**	**.004**	**.000**	**.000**
	n	423	206	217	116	303	71	45	135	168
On.Ar	*r*	-.345	-.327	-.317	-.252	-.372	-.156	-.160	-.424	-.324
	r^2	11.90%	10.69%	10.05%	6.35%	13.84%	2.43%	2.56%	17.98%	10.50%
	p	**.000**	**.000**	**.000**	**.011**	**.000**	.226	.332	**.000**	**.000**
	n	376	179	197	101	271	62	39	117	154
Ot.Dn	*r*	.354	.297	.357	.331	.352	.164	.446	.376	.317
	r^2	12.53%	8.82%	12.74%	10.96%	12.39%	2.69%	19.89%	14.14%	10.05%
	p	**.000**	**.000**	**.000**	**.002**	**.000**	.249	**.006**	**.000**	**.000**
	n	330	150	180	88	238	51	37	99	139

Table 4. Results from Reduced Major Axis (RMA) regression tests for all significant and "strongest" correlations as identified in Table 3 (also see Figure 2), where histology data are regressed against Ct.Wi.

RMA regression **x = Ct.Wi**	**Slope (*b*)**	**r^2**	**95% CI slope**	**intercept**	***p***	**Relationship** **b >1: positive allometry** **b = 1: isometric growth** **b <1: negative allometry**
y = N.On						
Young adults	1.075	0.073	0.840, 1.277	0.092	0.002	isometric growth
Young males	1.543	0.107	0.985, 4.980	-0.409	0.022	"
y = OPD						
Young males	1.060	0.230	0.690, 1.328	0.205	0.001	isometric growth
y = H.Ar						
Entire sample	-3.781	0.110	-4.106, -3.434	6.508	0.000	negative allometry
Females	-3.678	0.132	-4.085, -3.168	6.613	0.000	"
Males	-4.267	0.100	-4.800, -3.644	7.368	0.000	"
Middle-aged adults	-3.900	0.130	-4.282, -3.438	6.950	0.000	"
Middle-aged females	-3.905	0.256	-4.432, -3.262	6.849	0.000	"
Middle-aged males	-4.113	0.096	-4.674, -3.450	7.243	0.000	"
y = H.Dm						
Entire sample	-1.736	0.159	-1.887, -1.574	3.292	0.000	negative allometry
Females	-1.667	0.198	-1.863, -1.448	3.192	0.000	"
Males	-1.963	0.124	-2.215, -1.669	3.547	0.000	"
Young adults	-1.555	0.169	-1.763, -1.291	3.096	0.000	"
Middle-aged adults	-1.816	0.156	-2.001, -1.601	3.380	0.000	"
Young males	-1.754	0.163	-2.139, -1.196	3.326	0.004	"
Middle-aged females	-1.716	0.281	-1.960, -1.423	3.247	0.000	"
Middle-aged males	-1.970	0.113	-2.277, -1.596	3.561	0.000	"
y = On.Ar						
Entire sample	-2.944	0.110	-3.209, -2.625	7.149	0.000	negative allometry
Females	-3.261	0.092	-3.723, -2.713	7.362	0.000	"
Males	-3.045	0.121	-3.394, -2.650	7.315	0.000	"
Middle-aged adults	-3.060	0.121	-3.392, -2.673	7.276	0.000	"
Middle-aged females	-3.556	0.148	-4.231, -2.769	7.644	0.000	"
Middle-aged males	-2.965	0.124	-3.312, -2.517	7.249	0.000	"
y = Ot.Dn						
Entire sample	1.604	0.137	1.431, 1.755	1.273	0.000	positive allometry
Females	1.535	0.107	1.250, 1.767	1.372	0.000	"
Males	1.825	0.137	1.562, 2.056	1.026	0.000	"
Young adults	1.609	0.177	1.211, 1.892	1.297	0.000	"
Middle-aged adults	1.601	0.122	1.410, 1.770	1.264	0.000	"
Young males	2.081	0.291	1.362, 2.623	0.800	0.000	"
Middle-aged females	1.516	0.166	1.217, 1.751	1.384	0.000	"
Middle-aged males	1.745	0.108	1.445, 1.994	1.095	0.000	"

Table 5. Results from reduced major axis (RMA) regression tests for all significant and "strongest" correlations as identified in Table 4 (also see Figure 3), where histology data are regressed against Ct.Wi.RI.

RMA regression **x = Ct.Wi.RI**	**Slope (*b*)**	r^2	**95% CI slope**	**intercept**	***p***	**Relationship** **b > 1: positive allometry** **b = 1: isometric growth** **b < 1: negative allometry**
x = N.On						
Young adults	1.124	0.060	0.815, 1.366	0.752	0.007	isometric growth
Young males	1.390	0.049	0.696, 4.457	0.638	0.162	"
x = OPD						
Young adults	0.892	0.109	0.678, 1.070	0.960	0.000	isometric growth
Young males	0.883	0.100	0.410, 1.191	0.949	0.045	"
x = H.Ar						
Entire sample	-3.890	0.125	-4.240, -3.497	4.407	0.000	negative allometry
Females	-3.553	0.148	-3.964, -3.046	4.280	0.000	"
Males	-4.236	0.105	-4.772, -3.580	4.545	0.000	"
Young adults	-3.568	0.094	-4.156, -2.757	4.283	0.000	"
Middle-aged adults	-3.969	0.135	-4.389, -3.507	4.444	0.000	"
Middle-aged females	-3.696	0.229	-4.186, -3.132	4.329	0.000	"
Middle-aged males	-4.171	0.093	-4.783, -3.398	4.536	0.000	"
x = H.Dm						
Entire sample	-1.783	0.170	-1.952, -1.593	2.190	0.000	negative allometry
Females	-1.635	0.205	-1.840, -1.400	2.141	0.000	
Males	-1.925	0.134	-2.177, -1.600	2.241	0.000	"
Young adults	-1.609	0.178	-1.866, -1.280	2.132	0.000	"
Middle-aged adults	-1.844	0.164	-2.034, -1.560	2.212	0.000	"
Young females	-1.637	0.124	-1.980, -1.213	2.134	0.003	"
Young males	-1.626	0.180	-2.042, -0.935	2.146	0.003	"
Middle-aged females	-1.642	0.261	-1.887, -1.350	2.147	0.000	"
Middle-aged males	-2.033	0.087	-2.327, -1.663	2.275	0.000	"
x = On.Ar						
Entire sample	-2.986	0.103	-3.274, -2.643	5.266	0.000	negative allometry
Females	-3.081	0.092	-3.526, -2.546	5.269	0.000	"
Males	-2.968	0.104	-3.342, -2.521	5.283	0.000	"
Middle-aged adults	-3.098	0.122	-3.425, -2.682	5.304	0.000	"
Middle-aged females	-3.437	0.123	-4.083, -2.620	5.371	0.000	"
Middle-aged males	-2.994	0.081	-3.390, -2.523	5.291	0.000	"
x = Ot.Dn						
Entire sample	1.611	0.112	1.416, 1.782	2.303	0.000	positive allometry
Males	1.718	0.114	1.429, 1.953	2.267	0.000	"
Young adults	1.633	0.100	1.130, 2.001	2.300	0.004	"
Middle-aged adults	1.595	0.113	1.385, 1.775	2.307	0.000	"
Young males	1.754	0.131	0.833, 2.330	2.262	0.029	"
Middle-aged females	1.418	0.145	1.177, 1.626	2.365	0.000	"
Middle-aged males	1.805	0.090	1.471, 2.064	2.231	0.000	"

Supplement Table 1. Descriptive data for ratio values of histology variables.

Grouping	***Histology variable ratio***	**N**	**Min**	**Max**	**Mean**	**SD**
Entire sample	H.Ar: On.Ar	401	.007	.670	.0889	.0621
	N.On: OPD	413	.293	1.093	.719	.078
	Ot.Dn: OPD	351	10.222	95.731	35.113	11.352
	Ot.Dn: On.Ar	351	.004	.403	.0386	.0390
Females	H.Ar: On.Ar	190	.007	.670	.086	.0618
	N.On: OPD	193	.467	1.093	.729	.0740
	Ot.Dn: OPD	160	10.971	95.731	34.838	11.241
	Ot.Dn: On.Ar	161	.004	.403	.0345	.0426
Males	H.Ar: On.Ar	211	.026	.618	.091	.062
	N.On: OPD	220	.293	.856	.710	.081
	Ot.Dn: OPD[1]	191	10.222	67.895	35.343	11.470
	Ot.Dn: On.Ar	190	.004	.217	.0420	.0355
Young adults	H.Ar: On.Ar	110	.007	.220	.0817	.0403
	N.On: OPD	116	.293	.889	.730	.0849
	Ot.Dn: OPD	95	10.971	95.731	39.203	13.191
	Ot.Dn: On.Ar	94	.006	.130	.0363	.0282
Middle-aged adults	H.Ar: On.Ar	286	.023	.670	.0917	.0683
	N.On: OPD	292	.418	1.093	.714	.0752
	Ot.Dn: OPD	251	10.222	65.641	33.574	10.212
	Ot.Dn: On.Ar	252	.004	.403	.0385	.0410
Old adults	H.Ar: On.Ar	5	.029	.231	.079	.085
	N.On: OPD	5	.712	.812	.753	.037
	Ot.Dn: OPD	5	19.146	46.417	34.655	11.154
	Ot.Dn: On.Ar	5	.010	.217	.086	.078
Young females	H.Ar: On.Ar	68	.007	.194	.081	.039
	N.On: OPD	70	.501	.889	.730	.081
	Ot.Dn: OPD	57	10.971	95.731	37.148	14.622
	Ot.Dn: On.Ar	57	.006	.118	.028	.022
Middle-aged females	H.Ar: On.Ar	121	.023	.670	.090	.072
	N.On: OPD	122	.467	1.093	.728	.070
	Ot.Dn: OPD[1]	102	19.160	60.817	33.700	8.580
	Ot.Dn: On.Ar	103	.004	.403	.038	.050
Old females	H.Ar: On.Ar	1	.047	.047	.047	N/A
	N.On: OPD	1	.758	.758	.758	
	Ot.Dn: OPD	1	19.146	19.146	19.146	
	Ot.Dn: On.Ar	1	.010	.010	.010	
Young males	H.Ar: On.Ar	42	.026	.220	.0835	.043
	N.On: OPD	46	.293	.846	.730	.091
	Ot.Dn: OPD[2]	38	26.046	67.895	42.285	10.110
	Ot.Dn: On.Ar	37	.009	.130	.049	.0319
Middle-aged males	H.Ar: On.Ar	165	.027	.618	.093	.066
	N.On: OPD	170	.418	.856	.704	.078
	Ot.Dn: OPD[1]	149	10.222	65.641	33.487	11.220
	Ot.Dn: On.Ar	149	.004	.182	.039	.033
Old males	H.Ar: On.Ar	4	.029	.231	.087	.097
	N.On: OPD	4	.712	.812	.752	.043
	Ot.Dn: OPD	4	29.396	46.417	38.532	8.103
	Ot.Dn: On.Ar	4	.057	.217	.104	.076

[1] Normally distributed data in this grouping (Kolmogorov-Smirnov normality test $p > .05$)

[2] Normally distributed data in this grouping (Shapiro-Wilk normality test $p > .05$)

Supplement Table 2. Results from Spearman's and Pearson's ([1]) correlation tests evaluating histomorphometry ratio data against posterior cortical width (Ct.Wi), and posterior cortical width robusticity index (Ct.Wi.RI). Underlined r^2 results indicate weak to moderate correlations, whereas the *p* values in bold indicate statistical significance < 0.05.

Ratio histology variable correlated with Ct.Wi	**Statistic**	**Entire Sample**	**Females**	**Males**	**Young adults**	**Middle-aged adults**	**Young females**	**Young males**	**Middle-aged females**	**Middle-aged males**
H.Ar: On.Ar	*r*	-.132	-.183	-.134	-.137	-.140	-.080	-.252	-.251	-.100
	r^2	1.74%	3.35%	1.80%	1.88%	1.96%	0.64%	6.35%	6.30%	1%
	p	**.008**	**.011**	.052	.153	**.018**	.515	.107	**.005**	.200
	n	401	190	211	110	286	68	42	121	165
N.On: OPD	*r*	.139	.131	.182	.148	.144	.114	.091	.153	.181
	r^2	1.93%	1.72%	3.31%	2.19%	2.07%	1.30%	0.83%	2.34%	3.28%
	p	**.000**	.069	**.007**	.112	**.014**	.349	.548	.092	**.018**
	n	351	193	220	116	292	70	46	122	170
Ot.Dn: OPD	*r*	.293	.281	.169[1]	.382	.272	.251	.411[1]	.268[1]	.220[1]
	r^2	8.58%	7.90%	2.86%	14.59%	7.40%	6.30%	16.89%	7.18%	4.84%
	p	**.000**	**.000**	**.032**	**.000**	**.000**	.060	**.010**	**.007**	**.007**
	n	351	160	160	95	251	57	38	102	149
Ot.Dn: On.Ar	*r*	.444	.349	.445	.409	.446	.172	.447	.439	.432
	r^2	19.71%	12.18%	19.80%	16.73%	19.89%	2.96%	19.98%	19.27%	18.66%
	p	**.000**	**.000**	**.000**	**.000**	**.000**	.201	**.006**	**.000**	**.000**
	n	351	161	190	94	252	57	37	103	149
Ratio histology variable correlated with Ct.Wi.RI										
H.Ar: On.Ar	*r*	-.174	-.196	-.161	-.200	-.159	-.095	-.362	-.235	-.097
	r^2	3.03%	3.84%	2.59%	4%	2.53%	0.90%	13.10%	5.52%	0.94%
	p	**.001**	**.009**	**.024**	**.044**	**.009**	.464	**.023**	**.011**	.232
	n	376	179	197	101	271	62	39	117	154
N.On: OPD	*r*	.154	.132	.180	.122	.166	.043	.112	.199	.164
	r^2	2.37%	1.74%	3.24%	1.49%	2.76%	0.18%	1.25%	3.96%	2.69%
	p	**.002**	.076	**.010**	.212	**.006**	.735	.480	**.030**	**.039**
	n	387	182	205	106	277	64	42	118	159
Ot.Dn: OPD	*r*	.246	.184	.082[1]	.240	.253	.090	.287[1]	.205[1]	.217[1]
	r^2	6.05%	3.39%	0.67%	5.76%	6.40%	0.81%	8.24%	4.11%	4.71%
	p	**.000**	**.025**	.317	**.025**	**.000**	.532	.089	**.043**	**.010**
	n	328	149	149	87	237	51	36	98	139
Ot.Dn: On.Ar	*r*	.387	.331	.380	.324	.399	.156	.306	.424	.371
	r^2	14.98%	10.96%	14.44%	10.50%	15.92%	2.43%	9.36%	17.98%	13.76%
	p	**.000**	**.000**	**.000**	**.002**	**.000**	.275	.073	**.000**	**.000**
	n	328	150	178	86	238	51	35	99	139

Supplement Table 3. Results from Reduced Major Axis (RMA) regression tests for all significant and "strongest" correlations identified in Supplement Table 2, where histology ratio data are regressed against Ct.WI and Ct.WI.RI.

RMA regression **x = Ct.Wi**	**Slope (*b*)**	r^2	**95% CI slope**	**intercept**	***p***	**Relationship** **b > 1: positive allometry** **b = 1: isometric growth** **b < 1: negative allometry**
x = Ot.Dn: OPD						
Young adults	1.579	0.093	1.141, 1.934	0.090	0.003	positive allometry
Young males	1.601	0.156	0.945, 2.041	0.019	0.017	isometric growth
x = Ot.Dn: On.Ar						
Entire Sample	4.235	0.156	3.783, 4.626	-5.589	0.000	positive allometry
Females	4.455	0.107	3.642, 5.110	-5.696	0.000	"
Males	4.549	0.173	3.884, 5.103	-5.987	0.000	"
Young adults	3.784	0.151	2.986, 4.934	-5.115	0.000	"
Middle-aged adults	4.353	0.154	3.806, 4.822	-5.726	0.000	"
Young males	4.765	0.189	2.945, 5.983	-6.146	0.007	"
Middle-aged females	4.884	0.161	3.801, 5.741	-6.097	0.000	"
Middle-aged males	4.366	0.162	3.693, 4.921	-5.820	0.000	"
RMA regression y = Ct.Wi.RI						
x = H.Ar: On.Ar						
Young males	-2.621	0.153	-3.327, -1.353	-0.242	0.014	negative allometry
x = Ot.Dn: On.Ar						
Entire Sample	4.303	0.133	3.802, 4.723	-2.881	0.000	positive allometry
Females	4.272	0.099	3.520, 4.941	-2.858	0.000	"
Males	4.365	0.143	3.664, 4.916	-2.912	0.000	"
Young adults	3.826	0.086	2.806, 4.591	-2.744	0.006	"
Middle-aged adults	4.403	0.147	3.868, 4.897	-2.912	0.000	"
Middle-aged females	4.614	0.160	3.694, 5.415	-2.945	0.000	"
Middle-aged males	4.311	0.137	3.544, 4.891	-2.905	0.000	"

Figure 1

Click here to download Figure Figure 1 final.tif

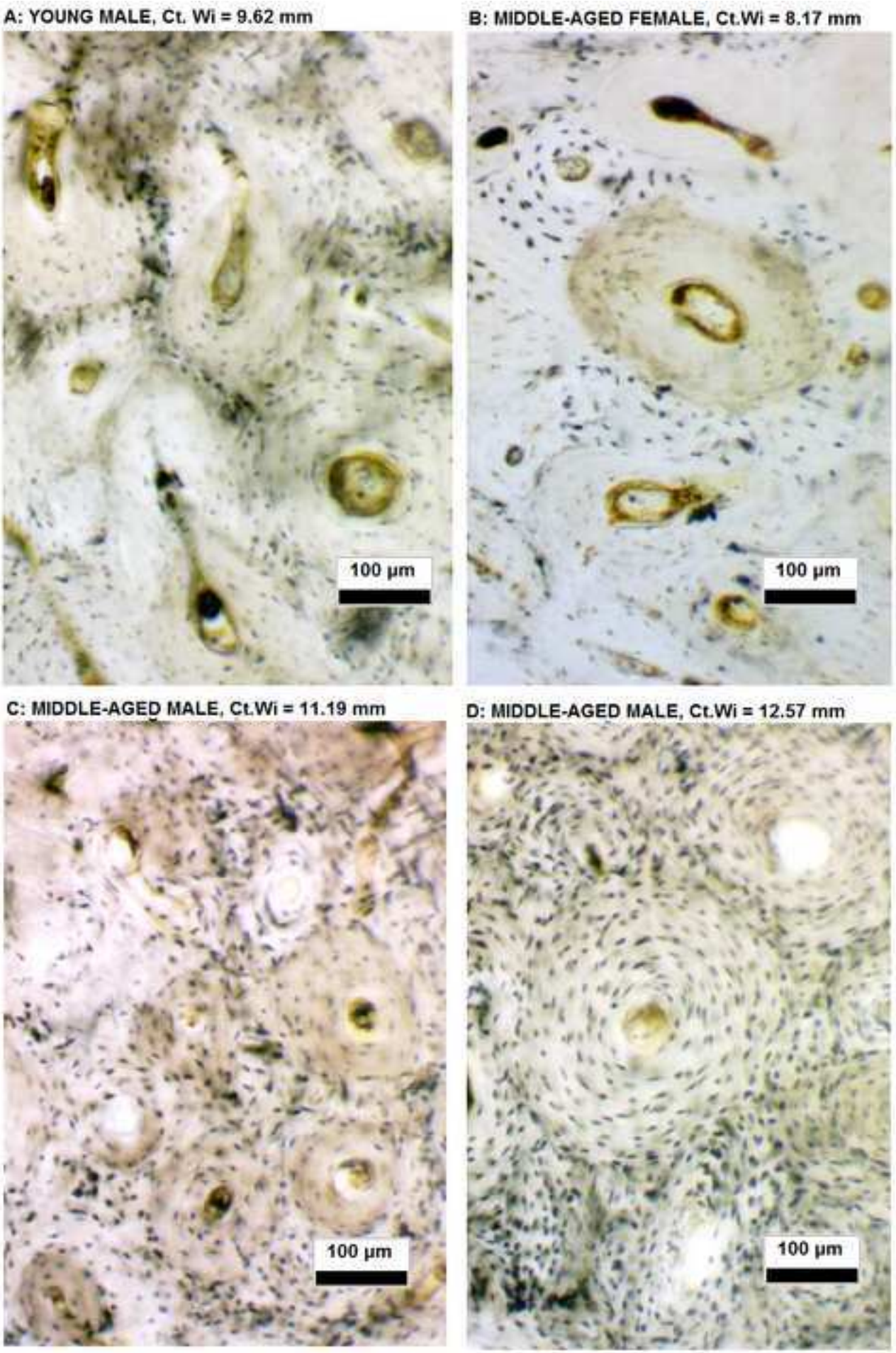

Figure 2

Click here to download Figure Figure 2.tif

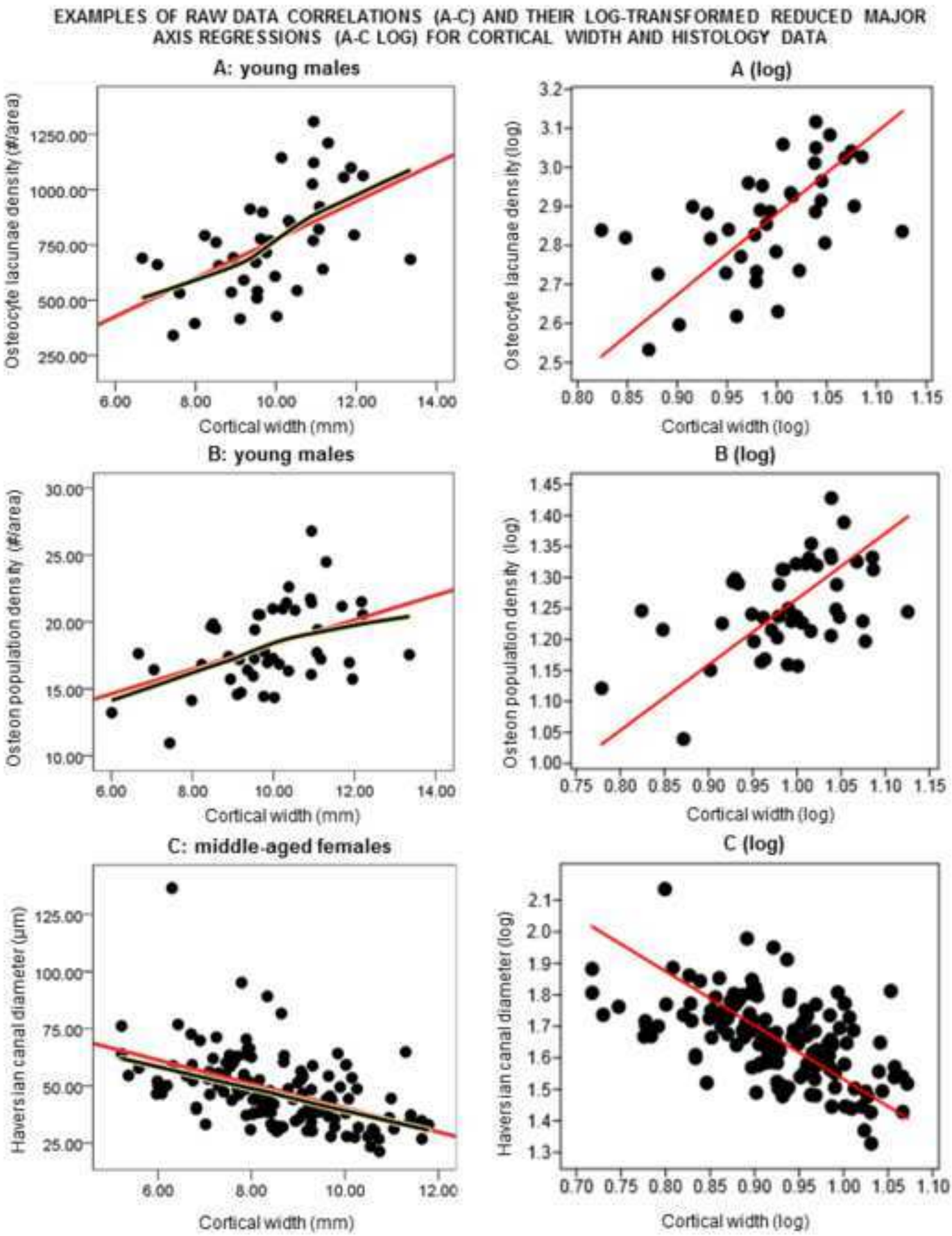

Figure 3

Click here to download Figure Figure 3.tif

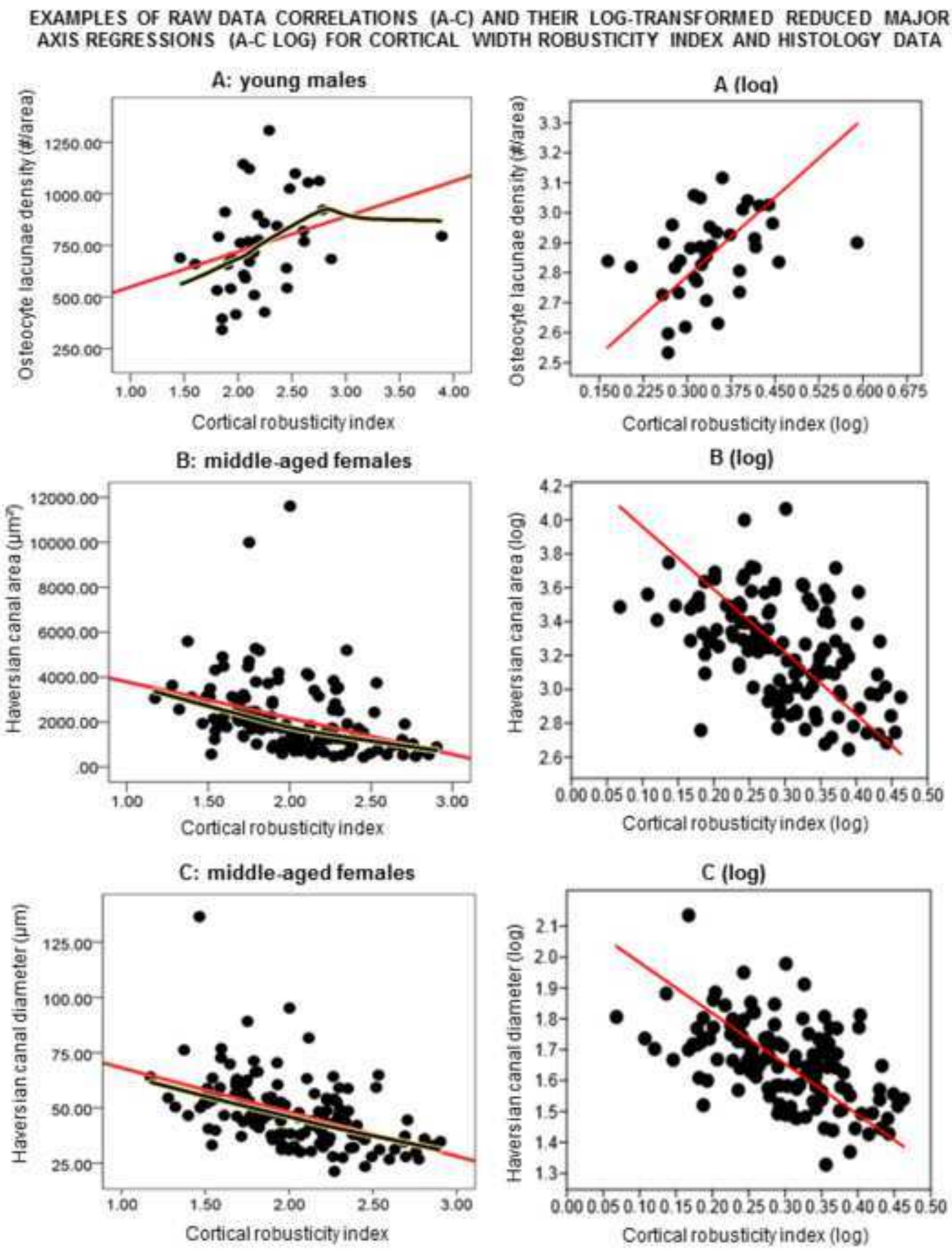

Figure 1.

A series of images illustrating variation (with age-at-death, sex, and measures of cortical width/ robusticity) in osteon and osteocyte lacunae densities, and Haversian canal and osteon size in the present sample of sub-periosteal posterior human midshaft femoral sections.

Figure 2.

A series of "strong" (see Table 2) simple correlations (raw data, A-C), and their log-transformed Reduced Major Axis regressions (A-C log, see Table 4), indicating negative and positive relationships between femoral cortical width and histology data.

Figure 3.

A series of "strong" (see Table 3) simple correlations (raw data, A-C), and their log-transformed Reduced Major Axis regressions (A-C log, see Table 5), indicating negative and positive relationships between femoral cortical width robusticity index and cortical histology data.